the process occurs after PrP^c reaches the plasma membrane, and it may involve the entry of PrP^c into intracellular acidic organelles [4–10].

As shown in Fig. 1A, the prion protein of the mouse, moPrP, consists of 208 amino acids (residues 23–231). It contains a carboxy-terminal domain, moPrP (121–231), which represents an autonomous folding unit with three α-helices (Helix1, Helix2, and Helix3) and a two-stranded antiparallel β-sheet [1–3,11–13]. In the full-length prion protein, moPrP (23–231), comparison of near-UV circular dichroism (CD), fluorescence and one-dimensional ^1H NMR spectra of moPrP (23–231) and moPrP (121–231) shows that amino-terminal segment 23–120, which includes the five characteristic octapeptide repeats, does not contribute measurably to the manifestation of the three-dimensional structure as detected [7]. Development of techniques for analysis of the structural and conformational changes in the amino-terminal region of moPrP is of great importance, because the amino-terminal region acts as a Cu^{2+} binding domain [11] and Cu^{2+} ions modulate various biological functions of prions such as the cellular enzymatic activity of superoxide dismutase (SOD) [14], signal transduction [15], shedding of PrP^c [16], and conversion to PrP^{sc} [17]. Recently, site-directed spin labeling (SDSL) together with electron spin resonance (ESR) spectroscopy has proven to be a practical method for determining the secondary structure and molecular orientation; surfaces of tertiary interactions; inter-residue distances and the chain topologies of various proteins [18–21]. SDSL involves the introduction of a spin-labeled side chain into protein sequences, usually through cysteine substitution mutagenesis, followed by reaction with a sulfhydryl-specific nitroxide reagent such as a methane thiosulfonate spin label (MTSSL) (Fig. 1B). Although SDSL-ESR is widely recognized as a useful method for structural analysis and domain dynamics of a number of membrane and soluble proteins, there are no reports about the application of this technique to detection of conformational changes in PrP^c.

In the present study, to obtain information about pH- and temperature-dependent conformational changes of typical domains in PrP, we employed the SDSL-ESR technique. We targeted the amino acid residues

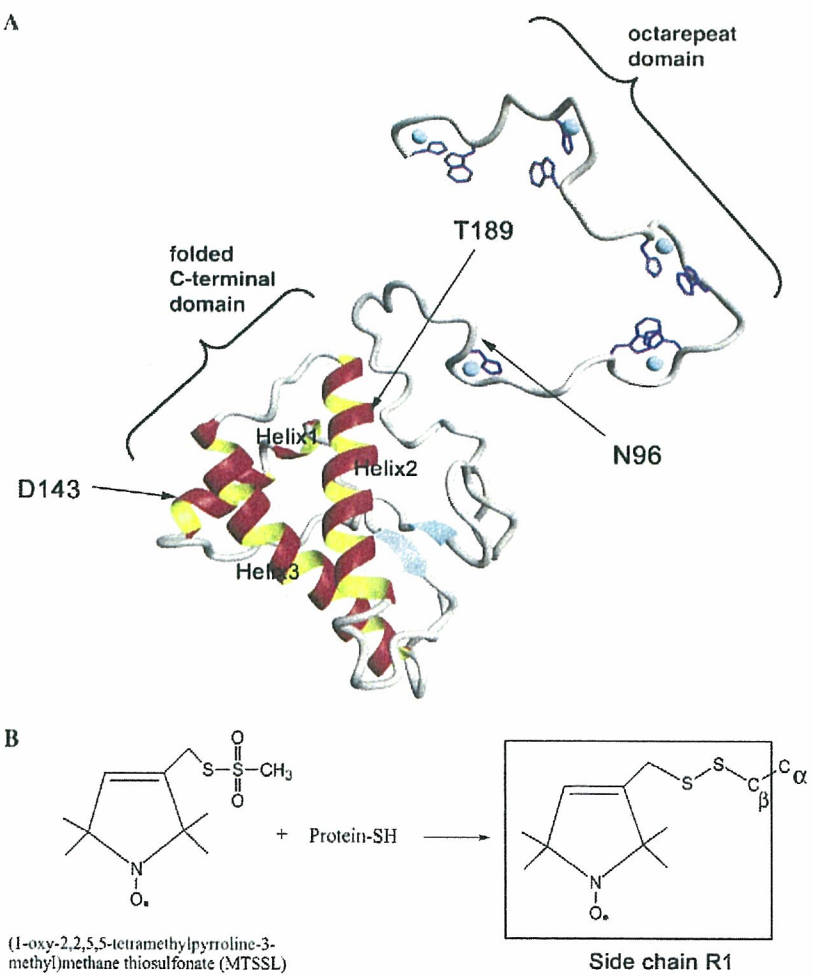

Fig. 1. (A) Three-dimensional rendering of PrP (61–231) [11] and the target sites (N96, D143, and T189) for site-directed spin-labeling (SDSL). (B) The reaction scheme of the methanethiosulfonate spin labeling reagent with cystein residue to yield the R1 side chain attached to the PrP.

of N96, D143, and T189 of recombinant moPrP for the SDSL study, since previous NMR studies have shown that N96, D143, and T189 in moPrP were localized in a Cu^{2+} binding region around H95, Helix1, and Helix2, respectively [7,12,13].

Materials and methods

Materials. (1-Oxy-2,2,5,5-tetramethyl-3-pyrroline-3-methyl)methanethiosulfonate (MTSSL) was purchased from Toronto Research Chemicals (ON, Canada). *Escherichia coli* BL21(DE3)*LysS* and isopropylthio-β-D-galactoside (IPTG) were from Invitrogen (CA, USA). The TSKgel Phenyl-5PW RP column was from TOSOH (Tokyo, Japan). Other reagents were from Wako Pure Chemical (Tokyo, Japan).

Construction of moPrP mutants. cDNA encoding moPrP codons 23–231 was cloned into *Bam*HI/*Eco*RI sites of pRSETb as described previously [22]. To generate the mutant moPrP containing a single amino acid substitution at codon 96 (Asn to Cys), 143 (Asp to Cys) or 189 (Thr to Cys), we used the PCR-based site-directed mutagenesis method described by Imai et al. [23]. The change of the codon by cystein substitution mutagenesis was confirmed using a DNA sequencer (CEQ8800, Beckman).

Expression and purification of recombinant moPrP mutants. The expression plasmids were introduced into *E. coli* BL21(DE3)*LysS*. Protein expression was induced by adding IPTG to a final concentration at 0.5 mM. Four to six hours after induction, bacterial cells were collected and inclusion bodies were prepared as described elsewhere [24]. The inclusion bodies from BL21(DE3)*LysS* transformed with expression plasmids were solubilized with 6 M GdnHCl in 20 mM phosphate buffer (pH 7.8). The recombinant moPrP was further purified by Ni^{2+}-immobilized metal affinity chromatography using Ni^{2+}-charged chelating Sepharose (Qiagen) and a stepwise elution gradient from pH 6.5 to 4.3 in the presence of 8 M urea. After dialysis against 10 mM acetate buffer (pH 4.0) for 48 h, recombinant moPrP containing an intramolecular disulfide bond was purified by reverse-phase HPLC using TSKgel phenyl-5PW RP and a 30–50% linear gradient of acetonitrile with 0.05% trifluoroacetic acid. The purified recombinant moPrP was dialyzed against 10 mM acetate buffer (pH 4.0) and stored at −20 °C until use. The protein concentration was determined by measuring the UV absorption at 276 nm using an extinction coefficient of 39,425 $cm^2\,M^{-1}$. Protein purity was analyzed by sodium dodecyl sulfate–polyacrylamide gel electrophoresis (SDS–PAGE), followed by Commasie brilliant blue staining. All mutants were at least 95% pure as judged by the SDS–PAGE.

Circular dichroism. Far-UV circular dichroism (CD) spectra were recorded on a JASCO J-820 spectropolarimeter with a protein concentration of 0.3 mg/ml in 1 mm pathlength cuvettes using a scan speed of 50 nm/min and a response time of 2 s. Multiple scans were averaged (typically $n = 6$).

Spin-labeling of moPrP mutants. To label the moPrP mutants with MTSSL, a 10-fold molar excess of MTSSL was added to each moPrP mutation in 10 mM acetate buffer (pH 4.5) and the sample was incubated in the dark for 12–24 h at 4 °C for solvent-accessible sites. The free spin label was removed from the protein using a microdialyzer (Nippon Genetics) and spin-labeled moPrP was concentrated by centrifugal concentrator (Vivascience). To confirm the site-specific spin-labeling for the cystein residue created by mutagenesis, the sample solution containing the spin-labeled moPrP mutant was digested for 3–24 h at 37 °C with 1 μg/ml trypsin (Promega) in 50 mM Tris–HCl, pH 8.0, 1 mM $CaCl_2$, and the fragment mass was examined with a matrix-assisted laser desorption ionization (MALDI) mass spectrometer (AutoFLEX, Bruker) equipped with a 337 nm laser source. In all mutants, there was an increase of about $m/z = 184$ by addition of a side chain (R1) of the labeling compound as expected if specifically incorporated MTSSL was detected in each fragment containing the substituted cystein (data not shown).

ESR spectroscopy. The pH change of the sample solution was carried out by dialysis of the sample against 10 mM acetate buffer from pH 4.0 to 6.0 or 10 mM Tris–HCl buffer from pH 6.5 to 8.0. For ESR spectroscopy, 70 μl of spin-labeled moPrP solution was placed into a quartz flat cell (RST-DVT05; 50 mm × 4.7 mm × 0.3 mm, Radical Research). Spectra were detected using a JEOL-RE X-band spectrometer (JEOL) connected with a cylindrical TE011 mode cavity (JEOL). All the ESR spectra were recorded at the temperature range of 5–60 °C maintained by a temperature controller (ES-DVT4, JEOL). We used a field modulation of 0.2 mT operating at 100 kHz, an incident microwave power of 5 mW, and a field sweep of 10 mT. Three field sweeps were averaged for each acquired spectrum by using the Win-Rad Radical Analyzer System (Radical Research). The rotational correlation time (τ) was reported by using the following equation described by Kivelson [25]:

$$\tau(\text{nsec}) = a_0 \delta H_{(0)} \left(\sqrt{h_{(0)}/h_{(+1)}} - 1 \right). \quad (1)$$

Here $\delta H_{(0)}$ is the width of the central peak of the nitroxide signal (in mT); $h_{(0)}$ and $h_{(+1)}$ are the lineheights of the spectral peaks for the quantum numbers of $M = 0$ and $+1$, and we employed a value of 6.5 for the constant a_0. The practical evaluation of τ was performed by the spin-label calculator system of the Win-Rad Radical Analyzer System (Radical Research).

Results

Spin-labeling of recombinant moPrP

For the SDSL-ESR experiment, refolding of recombinant moPrP mutants isolated from inclusion bodies of *E. coli.* was achieved by dialysis against 10 mM acetate buffer (pH 4.0) and the native form of moPrP was isolated by reverse-phase HPLC. The native form of recombinant moPrP is generally defined by the oxidative formation of its single disulfide bond (Cys178–Cys213) and characterized by a typical α-helical far-UV CD spectrum, with minima at 208 and 222 nm [7,26]. These two minima at 208 and 220 nm are reported to disappear if the disulfide bond between Cys179 and Cys214 is destroyed by mutagenesis or treatment with a reducing reagent such as DTT [26]. Therefore, we first recorded far-UV CD spectra of recombinant moPrP mutants in order to confirm that the α-helix content of recombinant moPrP mutants was similar to that of recombinant wild-type moPrP. Fig. 2 shows far-UV CD spectra obtained from wild-type, N96C, D143C, and T189C moPrP. Two minima, at about 208 and 220 nm, typical of mainly a helix structure protein, were clearly observed in all samples and there were no differences in the spectra between wild-type moPrP and moPrP mutants (N96C, D143C, and T189C). Moreover, SDS–PAGE with or without dithiothreitol (DTT) showed that no intermolecular disulfide linkage was produced in any moPrP mutant (data not shown). Therefore, our results indicated that the mutagenesis did not affect the α-helical structure of recombinant PrP by preferential forma-

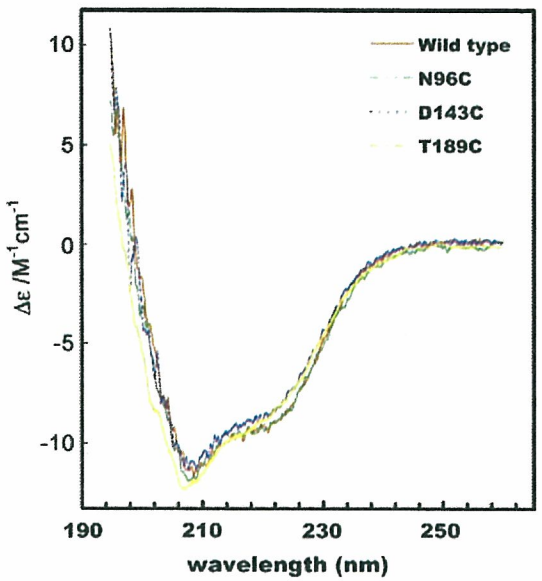

Fig. 2. Circular dichroism (CD) spectra obtained from 0.3 mg/ml moPrP (wild-type), moPrP (N96C), moPrP (D143C), and moPrP (T189C).

tion of a disulfide bond between Cys179 and Cys214, and that the cystein residue created by mutagenesis was preserved during the oxidative refolding.

Temperature-dependent conformational changes of moPrP

The ESR spectra detected from MTSSL bonded with moPrP (wild-type), moPrP (N96C), moPrP (D143C), and moPrP (T189C) are shown in Fig. 3. These ESR spectra are recorded at pH 7.4 at 20 °C. In PrP^c (wild-type), no signals derived from the nitroxide radical of MTSSL were detected, indicating that there were no free cystein residues, whereas a triplet ESR signal due to the nitroxide moiety undergoing various dynamic changes was clearly seen in moPrP (N96C), moPrP (D143C), and moPrP (T189C). The rotational correlation times (τ) of 1.1, 3.3, and 4.8 ns were evaluated from these ESR spectra of moPrP (N96C), moPrP (D143C), and moPrP (T189C), respectively. This indicated that the Cu^{2+} binding region was more flexible than the Helix1 region containing D139 or Helix2 containing T189. Furthermore, the line shapes of ESR spectra shown in Figs. 4A–C showed the temperature-dependent variation. There were some peaks in the outermost field of the ESR spectrum of T189R1 at 10 and 20 °C, which were due to the parallel component ($A_{\|}$) of the hyperfine tensor. These peaks, as shown by arrows in Fig. 4C, therefore indicated immobilization of the nitroxide moiety in the local region of T189R1. In fact, these peaks vanished at higher temperatures (e.g., 30 °C). The rotational correlation times (τ) were calculated and plotted as a function of temperature at pH 4.4, 6.4, and 7.4 in Figs. 4D–F. In all moPrP mutants, an increase of

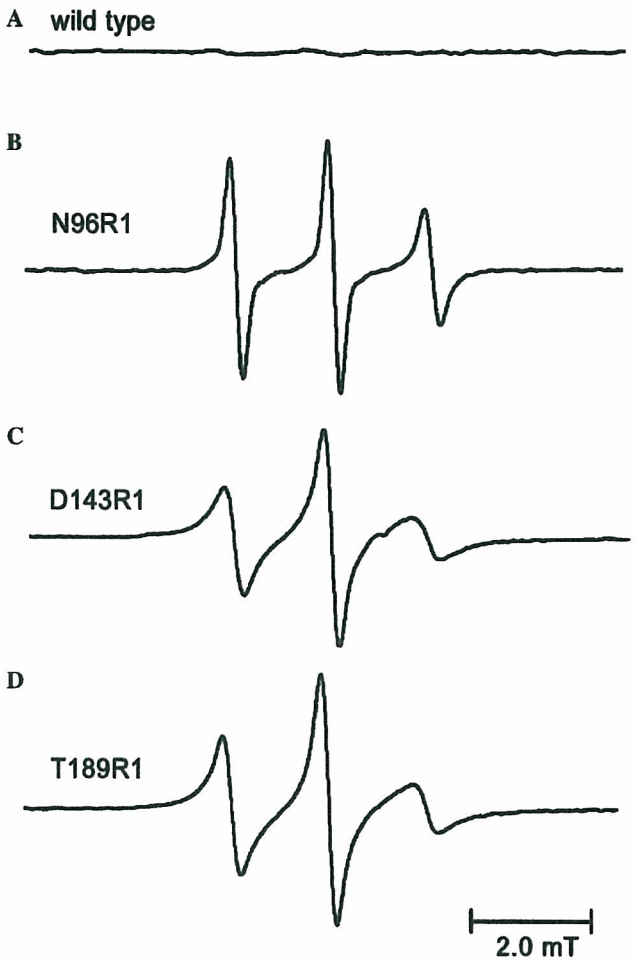

Fig. 3. X-band ESR spectra of spin-labeled recombinant moPrP mutants. After reaction of MTSSL with moPrP (wild-type) (A), moPrP (N96C) (B), moPrP (D143C) (C), and moPrP (T189C) (D), the free spin labeling compound was removed by dialysis against 10 mM acetate buffer (pH 4.0) for 48 h. pH of the sample was adjusted to 7.4 by dialysis against 10 mM Tris–HCl buffer for 4 ESR spectra were recorded by an X-band ESR spectrometer with a field modulation of 0.2 mT, operating at 100 kHz, an incident microwave power of 5 mW and a field sweep of 10 mT.

temperature induced a decrease in τ, which indicated rapid tumbling of the nitroxide moiety. Two phases, a steeper decline of τ at from 5 to 20 °C and a gentle decline at temperatures >20 °C, were observed in moPrP (D143C) and moPrP (T189C) at pH 4.4, 6.4, and 7.4. We found the presence of a breaking point or a phase transition at around 20 °C. The results of slower correlation times found at 10 and 20 °C explain the appearance of $A_{\|}$-peaks in the outermost field in moPrP (T189C). However, the phase transition point at 20 °C was not well defined in moPrP (N96C) at any pH.

pH-dependent conformational changes in moPrP

As shown in Fig. 4F, we found a difference in τ between pH 7.4 and 4.4 in moPrP (T189R1), although there were no pH-dependent differences in τ of moPrP

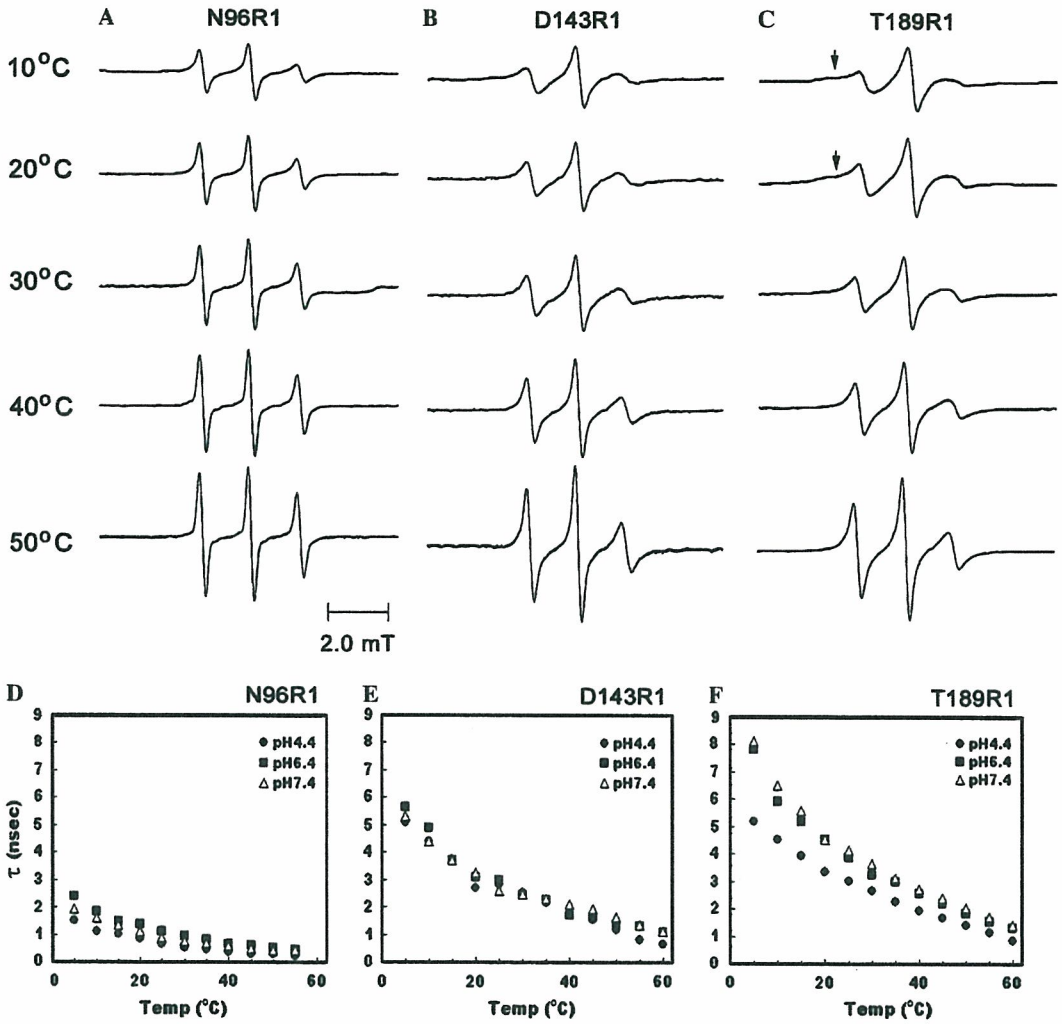

Fig. 4. X-band ESR spectra of recombinant moPrP (N96R1) (A), moPrP (D143R1) (B), and moPrP (T189R1) (C) at 10, 20, 30, 40, and 50 °C. The rotational correlation times, τ (ns), were evaluated from the ESR spectra of moPrP (N96R1) (D), moPrP (D143R1) (E), and moPrP (T189R1) (F) at various temperatures at pH 4.4, 6.4, and 7.4.

(N96C) and moPrP (D143C) as shown in Figs. 4D and E. Fig. 5 shows typical ESR spectra in pH 4.4 solution and pH 7.4 solution of moPrP (T189R1) recorded at 20 °C. The immobilization of the nitroxide moiety at pH 7.4 is obvious in comparison with that at pH 4.4. Furthermore, to define the pH-dependency, we examined the lineshape variation in the ESR spectra of moPrP (T189R1) and moPrP (T189R1) solutions whose pHs were gradually changed from pH 4.0 to 7.8 by dialysis. As shown in Fig. 5B, two regions were observable in moPrP (T189R1), a steep increase phase at pH 4.0–4.8 and a gradual increase phase at pH 5.4–7.8. Stone et al. [27] have also shown similar pH-dependent phase transition at around pH 4.0 in spin-labeled BSA. At temperatures from 5 °C to 20 °C, we found a breaking point between the two phases at around pH 5.0 that was clearer than those seen at temperatures >30 °C. These results indicated that the region around T189R1 was more pH-sensitive than the N96R1 and D189R1 regions.

Discussion

Preparation procedures of SDSL

Site-directed spin labeling is one of the most powerful methods for investigating the structure and conformational switching in soluble and membrane proteins [18,20]. Analysis of nitroxide side chain dynamics in spin-labeled proteins reveals contributions from fluctuations in the backbone, dihedral angles, and rigid-body motions of α-helices [18–21]. With this technique, however it is necessary that free cystein residues be substituted for alanine or serine residues for specificity in the reaction of MTSSL with the target cystein residue created by mutagenesis. The native mouse, hamster, bovine, and human prion proteins do not have free cystein residues, but a disulfide linkage is known to exist between Helix2 and Helix3, and to be essential for formation of three helix structures, which are important in refolding prion secondary structures [26].

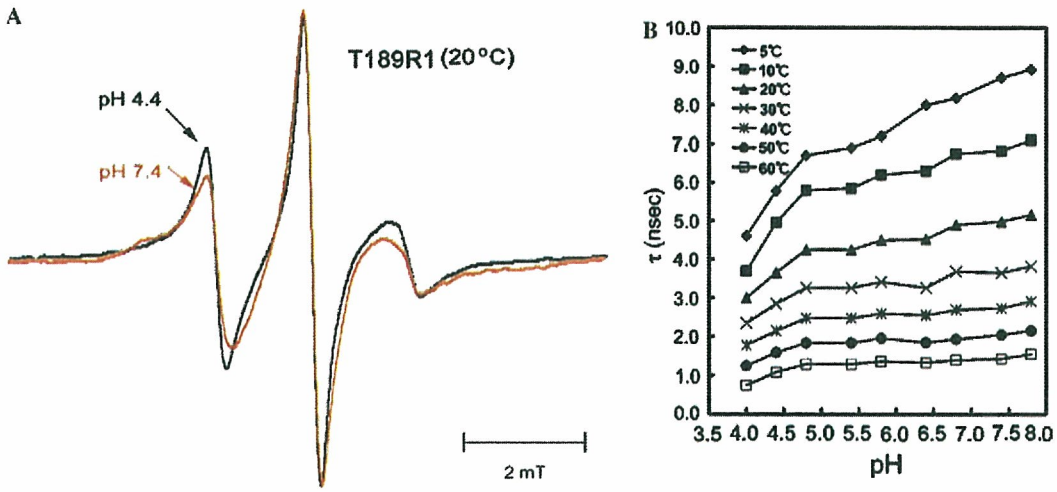

Fig. 5. (A) X-band ESR spectra of moPrP (T189R1) at 20 °C, and pH 4.4 (black line) and pH 7.4 (red line). (B) The rotational correlation time, τ (ns), at various pHs as detected by the ESR spectra of moPrP (T189R1) from 5 to 60 °C. (For interpretation of the references to colour in this figure legend, the reader is referred to the web version of this paper.)

Although Lundberg et al. [28] have reported the time-dependent changes of the ESR spectrum of a short synthetic prion-derived penta-peptide, AGAACAGA with Cys117 substituted for Ala117 in PrP (113–120), there have been few reports on structural analysis by SDSL for the full-length proteins such as PrP having an intracellular disulfide linkage. Application of the SDSL technique is impossible for full-length native PrP protein, because cystein residues newly created by mutagenesis interfere with the formation of the disulfide linkage between Helix2 and Helix3. For this reason, the present experiment employed dialysis against low pH buffer, and reverse-phase HPLC for the refolding and the purification procedures. We demonstrated that the recombinant moPrP produced by this preparation could be successfully used for SDSL experiments as proved by the following evidence. First, far-UV CD spectroscopy, as shown in Fig. 2, clearly demonstrated that the content of the helical structures in moPrP mutants was similar to that in native moPrP. This fact indicates the preferential formation of a disulfide linkage between Cys178 and Cys213, because the abrogation of this disulfide linkage never gives two minima at 208 and 220 nm in far-UV CD spectra [26]. Second, the possibility of dimer formation due to intermolecular disulfide-linkage between cystein residues newly created by mutagenesis was ruled out because SDS–PAGE of recombinant moPrP without the reducing reagent showed a single band (data not shown). Third, MALDI-TOF mass spectroscopic data showed increases of ca. $m/z = 184$ due to a side chain of the nitroxide moiety in the fragment after the tryptic digestion of spin-labeled moPrP mutants (data not shown). Thus, we were able to preserve the target cystein created by mutagenesis and succeeded for the first time in applying SDSL to the full-length prion protein.

Conformational changes of Cu^{2+} binding region and α-helix regions

Prion protein was reported to contain an amino-terminal Cu^{2+} binding octarepeat segment and a carboxy-terminal domain, three α-helices (Helix1, Helix2, and Helix3), and a two-stranded antiparallel β-sheet [1–3,11–13]. The amino acid residues of N96, D143, and T189 in moPrP have been chosen as targets for SDSL. Recently, in addition to the octapeptide repeat region, a novel Cu^{2+} binding structure between H95 and H110 was reported [29] and N96 is close to this region. D143 is located in the initial part of Helix1 and D189 in the end part of Helix2. A marked difference in rotational correlation times was observed by the spin-labeled positions (Fig. 3). NMR data of hamster PrP (90–231) showed that the region from 90 to 124, which includes the characteristic octapeptide repeat sequence, was clearly flexible with large negative NOEs and local correlation times of less than 1 ns. This is due to the fact that residues do not form part of any stable secondary or tertiary fold and are highly flexible [30]. Our ESR spectrum of moPrP (N96R1) also showed that the Cu^{2+} region around H95 reflected more flexible motion as compared with the rigid-body motion of helix structure revealed by ESR-lineshapes from moPrP (D143R1) and moPrP (T189R1).

Our data showed that the end part of Helix2 around T189R1 was highly pH-sensitive compared to the Cu^{2+} binding region around N96R1 and the first part of Helix1 around T189R1 (Figs. 4D–F and 5). The conversion from PrP^{c} to PrP^{Sc} is a post-transcriptional process that appears via the endosome pathway [4,5,9] and/or caveolae-like domains [10], both of which are acidic. Lower pH also accelerates conversion from

PrP^{c} to PrP^{Sc} in a cell-free system [31]. Recently, Swietnicki et al. [32] have shown that incubation of the recombinant prion protein under mildly acidic conditions (pH 5 or below) in the presence of low concentrations of guanidine hydrochloride produces a transition to PrP^{Sc}-like β-sheet-rich oligomers that show fibrillar morphology and increased resistance to proteinase K digestion. Since low pH plays a role in facilitating the conformational change that ultimately results in PrP^{Sc} formation, some parts of Helix2 may be candidates for the pH-sensitive region associated with PrP^{Sc} conversion. In this region, we found a phase transition point at around pH 5.0 as shown in Fig. 5B. This evoked the induction of rapid structural change in the end part of Helix2 below pH 5.0. For analysis of the precise mechanism of pH-induced conformational changes in this region, further studies using the SDSL-ESR technique using a variety of recombinant moPrP mutants created on Helix2 will be necessary.

ESR of spin label dynamics

The mobility of the spin label moiety attached to a protein can be quantified in terms of the rotational correlation times in the case of weakly immobilized labels ($\tau = 10^{-9}$–10^{-10} s). τ is determined by the relative linewidths based upon relaxation theory and is given by Eq. (1) (vide infra). In the equation, the lineheights are used instead of the linewidths, because the former are easy to measure accurately. The constant factor a_0 in Eq. (1) is derived from the g-factor and hyperfine anisotropies. For these reasons, Eq. (1) is only applicable to a spin label signal that possesses three well-defined lines with longitudinal (or up and down) symmetry and no anisotropic outermost lines due to the $g_{\|}$ anisotropy. In the present study, we applied Eq. (1) to the rapid tumbling of the weakly immobilized regime of the spin label dynamics.

Acknowledgments

This work was supported in part by Grants-in-Aid for Basic Scientific Research from the Ministry of Education, Culture, Sports, Science and Technology of Japan [No. 17380178 (O.I.), No. 17580275, and No. 17658126 (M.K.)]. O.I., Y.S., and H.N. thank the Research Grants from COE program and CREST-JST program.

References

[1] S.B. Prusiner, Prions, Proc. Natl. Acad. Sci. USA 95 (1998) 13363–13383.
[2] C. Weissmann, Molecular genetics of transmissible spongiform encephalopathies, J. Biol. Chem. 274 (1999) 3–6.
[3] A. Aguzzi, M. Glatzel, F. Montrasio, M. Prinz, F.L. Heppner, Interventional strategies against prion diseases, Nat. Rev. Neurosci. 2 (2001) 745–749.
[4] B. Caughey, G.J. Raymond, The scrapie-associated form of PrP is made from a cell surface precursor that is both protease- and phospholipase-sensitive, J. Biol. Chem. 266 (1991) 18217–18223.
[5] B. Caughey, G.J. Raymond, D. Ernst, R.E. Race, N-terminal truncation of the scrapie-associated form of PrP by lysosomal protease(s): implications regarding the site of conversion of PrP to the protease-resistant state, J. Virol. 65 (1991) 6597–6603.
[6] A. Taraboulos, M. Scott, A. Semenov, D. Avrahami, L. Laszlo, S.B. Prusiner, D. Avrahami, Cholesterol depletion and modification of COOH-terminal targeting sequence of the prion protein inhibit formation of the scrapie isoform, J. Cell Biol. 129 (1995) 121–132.
[7] S. Hornemanna, C. Korthb, B. Oeschb, R. Rieka, G. Widera, K. Wüthricha, R. Glockshubera, Recombinant full-length murine prion protein, mPrP (23–231): purification and spectroscopic characterization, FEBS Lett. 413 (1997) 277–281.
[8] A.C. Magalhaes, J.A. Silva, K.S. Lee, V.R. Martins, V.F. Prado, S.S. Ferguson, M.V. Gomez, R.R. Brentani, M.A. Prado, Endocytic intermediates involved with the intracellular trafficking of a fluorescent cellular prion protein, J. Biol. Chem. 277 (2002) 33311–33318.
[9] D.R. Borchelt, A. Taraboulos, S.B. Prusiner, Evidence for synthesis of scrapie prion proteins in the endocytic pathway, J. Biol. Chem. 267 (1992) 16188–16199.
[10] M. Vey, S. Pilkuhn, H. Wille, R. Nixon, S.J. DeArmond, E.J. Smart, R.G. Anderson, A. Taraboulos, S.B. Prusiner, Subcellular colocalization of the cellular and scrapie prion proteins in caveolae-like membranous domains, Proc. Natl. Acad. Sci. USA 93 (1996) 14945–14949.
[11] C.S. Burns, E. Aronoff-Spencer, G. Legname, S.B. Prusiner, W.E. Antholine, G.J. Gerfen, J. Peisach, G.L. Millhauser, Copper coordination in the full-length, recombinant prion protein, Biochemistry 42 (2003) 6794–6803.
[12] M. Billeter, R. Riek, G. Wider, S. Hornemann, R. Glockshuber, K. Wuthrich, Prion protein NMR structure and species barrier for prion diseases, Proc. Natl. Acad. Sci. USA 94 (1997) 7281–7285.
[13] R. Riek, S. Hornemann, G. Wider, M. Billeter, R. Glockshuber, K. Wuthrich, NMR structure of the mouse prion protein domain PrP (121–321), Nature 382 (1996) 180–182.
[14] W. Rachidi, D. Vilette, P. Guiraud, M. Arlotto, J. Riondel, H. Laude, S. Lehmann, A. Favier, Expression of prion protein increases cellular copper binding and antioxidant enzyme activities but not copper delivery, J. Biol. Chem. 278 (2003) 9064–9072.
[15] C. Spielhaupter, H.M. Schatzl, PrP^{C} directly interacts with proteins involved in signaling pathways, J. Biol. Chem. 276 (2001) 44604–44612.
[16] E.T. Parkin, N.T. Watt, A.J. Turner, N.M. Hooper, Dual mechanisms for shedding of the cellular prion protein, J. Biol. Chem. 279 (2004) 11170–11178.
[17] N. Hijazi, Y. Shaked, H. Rosenmann, T. Ben-Hur, R. Gabizon, Copper binding to PrP^{C} may inhibit prion disease propagation, Brain Res. 993 (2003) 192–200.
[18] W.L. Hubbell, C. Altenbach, C.M. Hubbell, H.G. Khorana, Rhodopsin structure, dynamics, and activation: a perspective from crystallography, site-directed spin labeling, sulfhydryl reactivity, and disulfide cross-linking, Adv. Protein Chem. 63 (2003) 243–290.
[19] R. Biswas, H. Kuhne, G.W. Brudvig, V. Gopalan, Use of EPR spectroscopy to study macromolecular structure and function, Sci. Prog. 84 (2001) 45–67.
[20] W.L. Hubbell, D.S. Cafiso, C. Altenbach, Identifying conformational changes with site-directed spin labeling, Nat. Struct. Biol. 7 (2000) 735–739.

[21] H.S. Mchaourab, M.A. Lietzow, K. Hideg, W.L. Hubbell, Motion of spin-labeled side chains in T4 lysozyme. Correlation with protein structure and dynamics, Biochemistry 35 (1996) 7692–76704.
[22] C.L. Kim, A. Umetani, T. Matsui, N. Ishiguro, M. Shinagawa, M. Horiuchi, Antigenic characterization of an abnormal isoform of prion protein using a new diverse panel of monoclonal antibodies, Virology 320 (2004) 40–51.
[23] Y. Imai, Y. Mastushima, T. Sugimura, M. Terada, A simple and rapid method for generating a deletion by PCR, Nucleic Acid Res. 19 (1991) 2785.
[24] J. Sambrook, E.F. Fritsch, T. Maniatis, Molecular Cloning: A Laboratory Manual, Cold Spring Harbor Press, Cold Spring Harbor, NY, 1989.
[25] D. Kivelson, Theory of ESR linewidths of free radicals, J. Chem. Phys. 33 (1960) 1094–1106.
[26] N.R. Maiti, W.K. Surewicz, The role of disulfide bridge in the folding and stability of the recombinant human prion protein, J. Biol. Chem. 276 (2001) 2427–2431.
[27] T.J. Stone, T. Buckman, P.L. Nordio, H.M. McConnel, Spin-labeled biomolecules, Proc. Natl. Acad. Sci. USA 54 (1965) 1010–1017.
[28] K.M. Lundberg, C.J. Stenland, F.E. Cohen, S.B. Prusiner, G.L. Millhauser, Kinetics and mechanism of amyloid formation by the prion protein H1 peptide as determined by time-dependent ESR, Chem. Biol. 4 (1997) 345–355.
[29] C.E. Jones, S.R. Abdelraheim, D.R. Brown, J.H. Viles, Preferential Cu^{2+} coordination by His96 and His111 induces beta-sheet formation in the unstructured amyloidogenic region of the prion protein, J. Biol. Chem. 279 (2004) 32018–32027.
[30] H. Liu, S. Farr-Jones, N.B. Ulyanov, M. Llinas, S. Marqusee, D. Groth, F.E. Cohen, S.B. Prusiner, T.L. James, Solution structure of Syrian hamster prion protein rPrP (90–231), Biochemistry 38 (1999) 5362–5377.
[31] D.A. Kocisko, S.A. Priola, G.J. Raymond, B. Chesebro, P.T.Jr. Lansbury, B. Caughey, Species specificity in the cell-free conversion of prion protein to protease-resistant forms: a model for the scrapie species barrier, Proc. Natl. Acad. Sci. USA 92 (1995) 3923–3927.
[32] W. Swietnicki, M. Morillas, S.G. Chen, P. Gambetti, W.K. Surewicz, Aggregation and fibrillization of the recombinant human prion protein huPrP90–231, Biochemistry 39 (2000) 424–431.

Suppression of Proliferation of Poliovirus and Porcine Parvovirus by Novel Phenoxazines, 2-Amino-4,4α-dihydro-4α-7-dimethyl-3*H*-phenoxazine-3-one and 3-Amino-1,4α-dihydro-4α-8-dimethyl-2*H*-phenoxazine-2-one

Akiko IWATA,[a] Teruhide YAMAGUCHI,[a] Kouei SATO,[b] Noriko YOSHITAKE,[c] and Akio TOMODA*,[d]

[a] *Division of Cellular and Gene Therapy Products, National Institute of Health, Sciences; 1–18–1 Kamiyoga, Setagaya-ku, Tokyo 158–0098, Japan:* [b] *The Institute of Saitama Red Cross Cente; 8–3–41 Kamiochiai, Saitama, Saitama 338–0001, Japan:* [c] *Third Department of Internal Medicine, Tokyo Medical University; and* [d] *Department of Biochemistry and Intractable Immune System Disease Research Center, Tokyo Medical University; 6–1–1 Shinjuku, Tokyo 160–0022, Japan.*
Received October 7, 2004; accepted January 5, 2005

The present study aimed at investigating the antiviral effects of 2-amino-4,4α-dihydro-4α-7-dimethyl-3*H*-phenoxazine-3-one (Phx-1) and 3-amino-1,4α-dihydro-4α-8-dimethyl-2*H*-phenoxazine-2-one (Phx-2) on 6 representative viruses: poliovirus, porcine parvovirus, simian virus 40 (SV-40), herpes simplex virus-1 (HSV-1), Sindbis virus, and vesicular stomatitis virus (VSV). Phx-1 and Phx-2 suppressed the proliferation of poliovirus in Vero cells and that of porcine parvovirus in ESK cells at concentrations between 0.25 μg/ml and 2 μg/ml, when the cells were treated with Phx-1 and Phx-2 for 1 h and then inoculated with these viruses. The proliferation of the other viruses, SV-40, HSV-1, Sindbis virus, and VSV, in the host cells was not influenced by Phx-1 or Phx-2 at concentrations less than 20 μg/ml. The results suggest that Phx-1 and Phx-2 may be useful to prevent the proliferation of poliovirus and porcine parvovirus infection and may contribute to developing new antiviral drugs in future.

Key words phenoxazine; poliovirus; porcine parvovirus

The development of antiviral drugs has been undertaken in parallel with that of vaccines, so as to overcome viral infections. Vaccination has been adopted to prevent several viral infections due to poliovirus, poxvirus, influenza virus *etc.* However, the usefulness of the antiviral drugs discovered so far seems to be restricted by the adverse effects of the drugs and the appearance of drug-resistant viruses.[1,2]

On the other hand, Tomoda *et al.* found that relatively water-soluble phenoxazines were biosynthesized by the reaction of *o*-aminophenol and its derivatives with human and bovine hemoglobin.[3—5] Among these phenoxazines, 2-amino-4,4α-dihydro-4α-7-dimethyl-3*H*-phenoxazine-3-one (Phx-1) has been demonstrated to have anticancer activity.[6,7] It was also shown that Phx-1 exerts an immunosuppressive effect on the activated lymphocytes such as B cells and T cells[8,9] and the activated mast cells.[10] Therefore, it seems of interest to investigate the effects of water-soluble phenoxazines on the proliferation of viruses in the host cells. We briefly reported that the proliferation of poliovirus inoculated to Vero cells was inhibited by Phx-1.[11] This discovery prompted us to investigate the effects of water-soluble phenoxazines on various kinds of viruses, because there is a possibility that a new antiviral drug may be developed through such an investigation. The present manuscript deals with studies on the antiviral effects of Phx-1 and 2-amino-4,4α-dihydro-4α-7-dimethyl-3*H*-phenoxazine-3-one (Phx-2) on 6 representative viruses: poliovirus, porcine parvovirus, simian virus (SV-40), herpes simplex virus-1 (HSV-1), Sindbis virus, and vesicular stomatitis virus (VSV).

MATERIALS AND METHODS

Phx-1, Phx-2, Cells and Viruses Phx-1 and Phx-2 were prepared by reaction of bovine hemoglobin with 2-amino-5-methylphenol and 2-amino-4-methylphenol, respectively, as previously described.[4,5] The chemical structures of Phx-1 and Phx-2 are shown in Fig. 1. Phx-1 or Phx-2 was dissolved in dimethyl sulfoxide (DMSO) before use to reach a concentration of 20 mM, and then was diluted with α-minimum essential medium (α-MEM).

African green monkey kidney cells (Vero cells), were generously supplied by the Japanese Cancer Research Resources Bank (Tokyo, Japan). The ESK cells (embryonic swine kidney cells line)[12] were kindly donated by Dr. J. Koga (JCR Co., Japan).

Cells were maintained in α-MEM supplemented with 10% fetal calf serum (FCS, Sigma Co., Ltd., St. Louis, MO, U.S.A.), and 30 mg/l kanamycin sulfate RPMI 1640 medium containing 10% heat-inactivated FCS, at 37 °C under moisturized air containing 5% CO_2.

Poliovirus (strain Sabin 1) was also donated by Dr. Koga. Porcine parvovirus (strain 90HS), SV-40, Sindbis virus, and HSV-1 (strain F) were the generous donation of Dr. M. Kohase (National Institute of Infectious Diseases). VSV (strain NJ) was the gift of Dr. H. Kita (Suntory Center Institute, Japan).

The supernatants of Vero cells infected with poliovirus, HSV-1, Sindbis virus, and VSV were used as the virus samples. The supernatant of ESK cells infected with porcine parvovirus was used as the porcine parvovirus sample. CV-1 cells were infected with SV-40 virus, and then 5 d after infec-

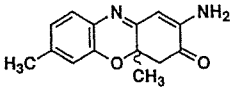

Phx-1

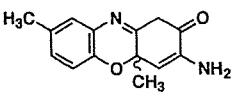

Phx-2

Fig. 1. Chemical Structures of Phx-1 and Phx-2

* To whom correspondence should be addressed. e-mail: tomoda@tokyo-med.ac.jp

Table 1. Effects of Phx-1 or Phx-2 on the Proliferation of Poliovirus Inoculated to Vero Cells at Different Concentrations of Phx-1 and Phx-2, Estimated by $TCID_{50}$[a]

	Phx-1 (μg/ml)					Phx-2 (μg/ml)				
	0	0.25	0.55	1	2	0	0.25	0.5	1	2
$TCID_{50}$	62	32	32	16	17	63	63	63	63	14

a) $TCID_{50}$ was defined as dilution ratio of the virus to generate 50% disruption of the cells.

tion, the supernatant was saved as the SV-40 sample. To remove the cell debris from the collected virus suspension, each suspension was centrifuged at 450×*g* for 10 min. After removing the debris, the resulting stock viruses were aliquoted and stored at −80 °C until use.

Determination of Viral Infectivity The infectious titer of virus suspension was determined using indicator cells. Poliovirus and porcine parvovirus were introduced into Vero cells and ESK cells, respectively.[13] The cells were seeded in a 96-well microplate (Asahi Technoglass Co., Ltd., Tokyo) at a density of 2×10^5 to 3×10^5 cells per well in culture medium. They were then cultured at 37 °C, for 2 d. Various concentrations of Phx-1 or Phx-2 solution [final concentration: 0 μg/ml (DMSO alone), 0.25, 0.5, 1 and 2 μg/ml] were then added to the cells in each well, and these were subsequently incubated for 1 h. After 1 h, the supernatant was removed from the well by an aspirator. At this time, poliovirus or porcine parvovirus which had been serially diluted with α-MEM to obtain a 50% tissue culture infectious dose ($TCID_{50}$, defined as dilution ratio of the virus to generate 50% disruption of the cells), as performed conventionally,[2] was added to Vero cells or ESK cells, respectively, in each well. Cell cultures were incubated for 1 h at 37 °C. Post infection $TCID_{50}$ cultures were then fed with α-MEM containing various concentrations of Phx-1 or Phx-2 [final concentration: 0 (DMSO alone), 0.25, 0.5, 1 and 2 μg/ml] and were incubated at 37 °C for 2 or 3 d.

After that period, the disruption of Vero cells or ESK cells was examined by the method described by Satoh *et al.*,[14] and the infectivity of poliovirus or porcine parvovirus to these cells was estimated. The estimation of the viruses SV-40, HSV-1, Sindbis virus and VSV was essentially in agreement with the method described by Satoh *et al.*[14]

Effects of Phx-1 and Phx-2 on Cell Viability We examined the effects of Phx-1 and Phx-2 on the viability of Vero cells, ESK cells, and CV-1 cells in the presence of various concentrations of these phenoxazines and without addition of viruses. There was no significant disruption of these cells at various concentrations of Phx-1 and Phx-2 up to 50 μg/ml, indicating that these phenoxazines do not affect the viability of the cells at the concentrations of used to examine the viruses.

RESULTS AND DISCUSSION

We initially studied the effects of Phx-1 and Phx-2 on the proliferation of poliovirus, a non-enveloped and single strand RNA virus, inoculated to Vero cells. Since $TCID_{50}$ is defined as the dilution ratio of the virus to generate 50% disruption of the cells, a lower value of $TCID_{50}$ means that the viral proliferation is being suppressed in the host cells. We found that

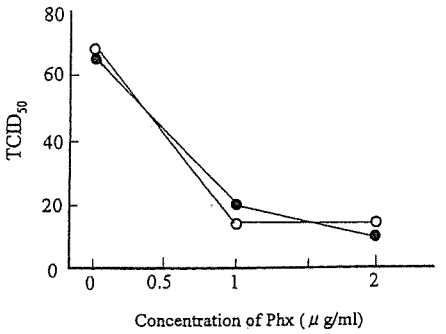

Fig. 2. Antiviral Effects of Phx-1 and Phx-2 on Porcine Parvovirus

The infectious titer of porcine parvovirus suspension was determined using ESK cells, as described in Materials and Methods. Antiviral effects of Phx-1 (●) or Phx-2 (○) were expressed by $TCID_{50}$ (defined as dilution ratio of the virus to generate 50% disruption of the cells) at different concentrations of these phenoxazines (μg/ml of Phx-1 or Phx-2).

$TCID_{50}$ of poliovirus was decreased according to the increase in the concentrations of Phx-1 or Phx-2 (Table 1). Namely, Phx-1 suppressed the proliferation of poliovirus inoculated to Vero cells at all concentrations tested between 0.25 μg/mg and 2 μg/ml, and reached maximal antiviral activity at 1 μg/ml. Phx-2 also inhibited the proliferation of poliovirus inoculated to Vero cells at 2 μg/ml (Table 1). Such inhibition was observed when the cells were treated with Phx-1 or Phx-2 for 1 h and then inoculated with poliovirus. On the contrary, the proliferation of poliovirus was not suppressed by Phx-1 or Phx-2 when Vero cells were inoculated with the virus together with various concentrations of Phx-1 or Phx-2 (data not shown). These results may be explained by the facts that these phenoxazines do not exert virucidal activity against poliovirus directly, but some mechanisms preventing the attachment or the intracellular proliferation of poliovirus in the host cells, are apparently revoked during 1 h incubation of the host cells with Phx-1 or Phx-2. The detailed biochemical changes in the host cells are not yet clear.

Figure 2 shows the inhibitory effects of Phx-1 and Phx-2 against porcine parvovirus, a non-enveloped and single strand DNA virus, as determined by the changes in $TCID_{50}$. These phenoxazines showed antiviral effects on porcine parvovirus at 1 μg/ml and 2 μg/ml. Such inhibition was observed when the cells were treated with Phx-1 or Phx-2 for 1 h and then inoculated with porcine parvovirus. However, Phx-1 or Phx-2 did not exert antiviral effects on porcine parvovirus when ESK cells were inoculated with the virus together with Phx-1 or Phx-2 (data not shown).

We studied the effects of Phx-1 and Phx-2 on various representative viruses such as SV-40 (non-enveloped, double strand DNA), HSV-1 (enveloped, double strand DNA), Sindbis virus (enveloped, single and plus strand RNA), and VSV (enveloped, single strand RNA). Table 2 summarizes the

Table 2. Antiviral Activity of Phx-1 and Phx-2 on Various Species of Viruses

Type of virus	Name of virus	Antiviral activity[a]	
		Phx-1	Phx-2
sDNA, envelope (−)	Porcine parvovirus	+	+
dDNA, envelope (−)	Simian virus 40	−	−
dDNA, envelope (+)	Herpes simplex virus-1	−	−
sRNA, envelope (−) (plus strand)	Poliovirus	+	+
sRNA, envelope (+) (plus strand)	Sindbis virus	−	−
sRNA, envelope (+) (minus strand)	Vesicular stomatitis virus	−	−

a) $TCID_{50}$ was estimated as described in Materials and Methods. Then, the antiviral activity was expressed by + or −, where + shows "effective" at the concentration of Phx-1 or Phx-2 between 0.25 and 20 μg/ml, and − shows "not effective" at these concentrations.

inhibitory effects of Phx-1 and Phx-2 on these viruses, in comparison with poliovirus and porcine parvovirus. Although Phx-1 and Phx-2 showed antiviral activity against poliovirus and porcine parvovirus, these phenoxazines did not inhibit the proliferation of SV-40, HSV-1, Sindbis virus or VSV in the host cells. Therefore, it may be conceivable that non-enveloped and single strand RNA virus (coxackie virus, ECHO virus, hepatitis virus A, encephalomyocarditis virus *etc.*) or non-enveloped and single strand DNA virus (B19 virus, adeno-associated virus 2 *etc.*) may be inhibited by Phx-1 and Phx-2 as well. Increased amounts of interferon is not possible, because the inhibition of proliferation of viruses was restricted only to poliovirus and porcine parvovirus (Table 2). These views should be assessed by further examinations.

Tang *et al.*[15] reported that hypericin, a derivative of emodin exerts antiviral activity against enveloped viruses such as HSV-1, influenza virus A and Mo-Mul V, but not against the non-enveloped viruses poliovirus and adenovirus, at concentrations of 1.56 to 25 μg/ml. On the other hand, our results showed that Phx-1 and Phx-2 exerted antiviral activity only against poliovirus and porcine parvovirus (Table 1, Fig. 2). Concerning the chemical structure of emodin (1,3,8-trihydroxy-6-methylanthraquinone) and Phx-1, emodin is analogous to Phx-1, because emodin and Phx-1 (Fig. 1) are tricyclic chromophores with the methyl group at the same position, however, the former is a semiquinone type producing active oxygens,[16] while the latter is a non-semiquinone type. Such similarity and differences in the chemical structure of these compounds may be reflected to the differences in biological actions between hypericin and Phx-1 or Phx-2.

Acknowledgments The present research was supported by funds from the Ito Foundation and from High-Tech Research Project for Private Universities: matching fund subsidy from the Ministry of Education, Culture, Sports, Science and Technology, Japan (2002—2006).

REFERENCES

1) Schaffer H. J., Beauchamp L., de Miranda P., Elion G. B., Bauer D. J., Collins P., *Nature* (London), **272**, 583—585 (1978).
2) Schmidtke M., Schnittler U., Jahn B., Dahse H., Stelzner A., *J. Virol. Methods*, **95**, 133—143 (2001).
3) Tomoda A., Yamaguchi J., Kojima H., Amemiya H., Yoneyama Y., *FEBS Lett.*, **196**, 44—48 (1986).
4) Tomoda A., Hamashima H., Arisawa M., Kikuchi T., Tezuka Y., Koshimura S., *Biochim. Biophys. Acta*, **1117**, 306—314 (1992).
5) Tomoda A., Arisawa M., Koshimura S., *J. Biochem.* (Tokyo), **110**, 1004—1007 (1991).
6) Mori H., Honda K., Ishida R., Nohira T., Tomoda A., *Anti-Cancer Drugs*, **11**, 653—657 (2000).
7) Koshibu-Koizumi J., Akazawa M., Iwamoto T., Takasaki M., Mizuno F., Kobayashi R., Abe A., Tomoda A., Hamatake M., Ishida R., *J. Cancer Res. Clin. Oncol.* **128**, 363—368 (2002).
8) Akazawa M., Koshibu-Koizumi J., Iwamoto T., Takasaki M., Nakamura M., Tomoda A., *Tohoku J. Exp. Med.*, **196**, 185—192 (2002).
9) Gao S., Takano T., Sada K., He J., Noda C., Hori-Tamura N., Tomoda A., Yamamura H., *Br. J. Pharmacol.*, **137**, 749—755 (2002).
10) Enoki E., Sada K., Qu X., Kyo S., Shahjahan Miah S. M., Hatani T., Tomoda A., Yamamura H., *J. Pharm. Sci.*, **94**, 329—333 (2004).
11) Iwata A., Yamaguchi A., Sato K., Izumi R., Tomoda A., *Tohoku J. Exp. Med.*, **200**, 161—165 (2003).
12) Kawamura H., Fujita T., Imada T., *Nippon Juigaku Zasshi*, **50**, 803—808 (1988).
13) Johnson K. L., Sarnow S. P., *J. Virol.*, **65**, 4341—4349 (1991).
14) Satoh K., Iwata A., Murata M., Hikata M., Hayakawa T., Yamaguchi T., *J. Virol. Methods*, **114**, 111—119 (2003).
15) Tang J., Colacino J. M., Larsen S. H., Spitzer W., *Antiviral Res.*, **13**, 313—326 (1990).
16) Huang H. C., Chu S. H., Chao P. D. L., *Eur. J. Pharmacol.*, **198**, 211—213 (1991).

NOTE *Clinical Pathology*

Polymorphisms of Caprine PrP Gene Detected in Japan

Yasuhisa KUROSAKI[1], Naotaka ISHIGURO[2]*, Motohiro HORIUCHI[3] and Morikazu SHINAGAWA[4]

[1]*Laboratory of Veterinary Public Health, Obihiro University of Agriculture and Veterinary Medicine, Obihiro, Hokkaido 080–8555,* [2]*Laboratory of Food and Environmental Hygiene, Faculty of Applied Biological Sciences, Gifu University, 1–1 Yanagido, Gifu 501–1193,* [3]*Laboratory of Prion Diseases, Graduate School of Veterinary Medicine, Hokkaido University, Sapporo 060–0818 and* [4]*Prion Disease Research Center, National Institute of Animal Health, 3–1–5 Kannondai, Tsukuba, Ibaragi 305–0856, Japan*

(Received 18 August 2004/Accepted 5 November 2004)

ABSTRACT. Polymorphism of the PrP gene is a primary factor influencing susceptibility and incubation period in natural and experimental scrapie in sheep and goats. Polymorphisms of the caprine PrP gene in Japan were examined in 118 goats. Eight allelic variants and 19 genotypes were obtained. Amino acid polymorphisms were observed at 7 codons: 102, 142, 143, 240, 127, 146 and 211 (the latter 3 are novel polymorphisms). The polymorphisms at codons 142M and 143R, which are associated with the resistance to scrapie, were relatively rare in the present study. Thus, the present results provide information about the caprine PrP gene that may be useful for assessing the risk of goat scrapie.

KEY WORDS: goat, polymorphism, PrP.

J. Vet. Med. Sci. 67(3): 321–323, 2005

Scrapie is a fatal and infectious neurodegenerative disease that occurs in sheep and goats. Like bovine spongiform encephalopathy (BSE) in cattle and Creutzfeld-Jakob disease (CJD) in humans, scrapie is a transmissible spongiform encephalopathy (TSE). TSEs are characterized by accumulation of an abnormal isoform (PrP^{Sc}) of a normal cellular prion protein (PrP^{C}) in the central nervous system [12].

Among animals with natural or experimental scrapie, there is considerable variation in susceptibility and incubation period, even when the animals are exposed to the same infectious agent simultaneously [1, 4, 9]. Studies have shown that interaction between the scrapie strain and the PrP genotype in the affected animals plays a primary role in differences in infectivity [4, 8]. Polymorphisms of the open reading frame (ORF) of the cellular PrP gene significantly influence the incidence of natural scrapie [1, 9]. Amino acid polymorphisms of the sheep PrP gene have been observed at the following codons: 112 (M→T), 136 (A→V), 137 (M→T), 138 (S→N), 141 (L→F), 151 (R→C), 154 (R→H), 171 (Q→H or Q→R), 176 (K→N), and 211 (R→Q). The amino acid polymorphism at codon 171 is strongly associated with incubation period in many breeds of sheep [1, 4, 7, 9, 10, 14].

Goats as well as sheep are natural hosts for scrapie. The clinical signs of affected goats are slightly different from those of sheep, but the observed variation of incubation period is similar to that described for sheep [11, 14]. Studies have shown amino acid polymorphisms of the caprine PrP gene at the following codons: 21 (V→A), 23 (L→P), 49 (G→S), 102 (W→G), 142 (I→M), 143 (H→R), 154 (R→H), 168 (P→Q), 220 (Q→H) and 240 (S→P) [2, 3, 5, 6, 11].

In Japan, caprine scrapie has not yet been observed, although occurrence of sheep scrapie in Japan has been reported [10, 13]. In the present study, we investigated polymorphisms of the PrP gene in goats raised in Japan, to obtain genetic information for use in assessing the risk of the occurrence of scrapie in goats.

A total of 118 samples (48 tonsillar samples and 70 blood samples) were collected from healthy goats in Japan (Table 1). The 48 tonsillar samples were collected from Honshu Island, the Hachijo Islands and Hokkaido Island for TSE surveillance. The 70 blood samples were collected from goats in the Hachijo Islands (32 samples) and Okinawa Island (38 samples). Most of the goats from which samples were obtained were of the Saanen breed or related breeds.

DNA extraction from the 48 tonsillar samples and 70 blood samples was performed using the DNeasy Tissue Kit and QIAamp DNA Blood Mini Kit (QIAGEN Science, MD), respectively.

For polymerase chain reaction (PCR) and sequencing of the caprine PrP gene, the sheep primer sets SPrP-1/SP-4 and SP-1/SPrP-2 were used to amplify the upstream region (approximately 430 bp) and downstream region (approximately 370 bp) of the PrP gene, respectively [7]. The over-

Table 1. Sampling sites and caprine PrP allele variations

Sampling Sites	Number of goats	PrP allelic variants (%)
Hokkaido Island	1	1(50), 8(50)
Honshu Island	6[a)]	1(42), 2(25), 6(8), 8(25)
Hachijyo Island	73	1(44), 2(38), 5(2), 6(1), 8(15)
Okinawa Island	38	1(34), 2(33), 3(3), 4(1), 5(11), 6(8), 7(5), 8(5)

a)Aomori prefecture (3 samples), Miyagi prefecture (1 sample), Hiroshima prefecture (1 sample) and Tokyo (1 sample).

* CORRESPONDENCE TO: Dr. ISHIGURO, N., Laboratory of Food and Environmental Hygiene, Faculty of Applied Biological Sciences, Gifu University, 1–1 Yanagido, Gifu 501–1193, Japan.

Table 2. Variations of caprine PrP gene

Allele	PrP codon[a]							Number
	102	127	142	143	146	211	240	goats
1[b]	W	G	I	H	N	R	S	99
2	–	–	–	–	–	–	P	82
3	G	–	–	–	–	–	–	2
4	–	S	–	–	–	–	P	1
5	–	–	M	–	–	–	P	11
6	–	–	–	R	–	–	P	7
7	–	–	–	–	S	–	P	4
8	–	–	–	–	–	Q	–	30
Total								236
Genotype								
1/1	WW	GG	II	HH	NN	RR	SS	22
1/2	WW	GG	II	HH	NN	RR	SP	31
2/2	WW	GG	II	HH	NN	RR	PP	17
1/3	WG	GG	II	HH	NN	RR	SS	1
2/3	WG	GG	II	HH	NN	RR	SP	1
2/4	WW	GS	II	HH	NN	RR	PP	1
1/5	WW	GG	IM	HH	NN	RR	SP	4
5/8	WW	GG	IM	HH	NN	RQ	SP	1
2/5	WW	GG	IM	HH	NN	RR	PP	3
5/5	WW	GG	MM	HH	NN	RR	PP	1
5/6	WW	GG	IM	HR	NN	RR	PP	1
1/6	WW	GG	II	HR	NN	RR	SP	5
1/2	WW	GG	II	HR	NN	RR	PP	3
6/7	WW	GG	II	HR	NS	RR	PP	1
1/7	WW	GG	II	HH	NS	RR	SP	2
2/7	WW	GG	II	HH	NS	RR	PP	1
1/8	WW	GG	II	HH	NN	RQ	SS	9
2/8	WW	GG	II	HH	NN	RQ	SP	8
8/8	WW	GG	II	HH	NN	QQ	SS	6
Total								118

a) Amino acids are described as the single letter: W,tryptohan; G, glycine; S, serine; I, isoleucine; M, methionine; H, histidine; R, arginine; N, asparagine; Q, glutamine acid; P, proline.
b) Wild type of sheep.

lapping region of the 2 amplified fragments was approximately 40 bp. PCR amplification and DNA sequencing were performed as described previously [7]. To verify novel polymorphisms of the caprine PrP gene detected by direct sequencing, cloning of the caprine PrP gene to a vector plasmid was performed as described previously [7]. Five colonies possessing the recombinant plasmid were selected, and their plasmid DNAs were prepared using a Plasmid Mini Kit (QIAGEN Science) and sequenced as described previously [7].

Nine polymorphisms of the DNA sequence of the caprine PrP gene were detected (Table 2). Two of those polymorphisms (at codons 42 and 138) were silent mutations, and the remaining 7 polymorphisms (at codons 102, 127, 142, 143, 146, 211 and 240) caused amino acid changes. Three of the amino acid substitutions detected in the present study were novel polymorphisms: at codon 127, a g→a nucleotide substitution in the first codon position caused an amino acid change of G→S; at codon 146, an a→g nucleotide substitution in the second position caused an amino acid change of N→S; at codon 211, a g→a nucleotide substitution caused an amino acid change of R→Q. The remaining 4 amino acid polymorphisms detected in the present study have previously been described: codon 102, W→G; codon 142, I→M; codon 143, H→R; codon 240, S→P [2, 5, 6, 11].

The present distinctive amino acid polymorphisms at 7 codons comprised 8 allelic variations and 19 different genotypes (Table 2). Alleles 1 and 2 are the predominant alleles of the caprine PrP gene in Japan. Genotype 1/1 has been identified in wild-type sheep in Japan, and genotypes 1/2 and 2/2 are commonly observed in goats in Japan. These 3 genotype groups are distinguished by alteration of codon 240, and accounted for 59% of the 118 present samples.

To estimate the genetic background of goats from Okinawa, Hachijo, Honshu and Hokkaido Islands, allelic variants were classified along with the sampling sites (Table 1). All allelic variations detected in the present study occurred in goats from Okinawa Island. Goats from Honshu and the Hachijo Islands possessed 2 major alleles (1 and 2) and the minor alleles 5, 6 and 8. Goats in Okinawa Island have been frequently introduced from several prefectures in Honshu Island, so that allelic variants were obviously detected.

However, there have been no recent introductions of new populations of goats to the Hachijo Islands (data not shown).

The structure of the caprine PrP gene is highly homologous to that of the sheep PrP gene, including exons, the promoter region and 256 amino acids [5]. In the ORF of the PrP gene, amino acid polymorphisms associated with incubation period differ between sheep and goats. Polymorphisms at codons 142 and 143 in goats are thought to influence the incubation period of scrapie in experimental challenges [5] and natural cases [2]. Few of the goats in the present study carried polymorphisms at codons 142M or 143R (Table 2), which are associated with the resistance to scrapie. Identification of caprine PrP genotype may provide information that can be used to select scrapie-resistant goat for breeding. No scrapie has been found in goats in Japan, and PrP^{Sc} has not been found in Japan by TSE surveillance using Western blot analysis (unpublished data). Although the number of goats examined in the present study was relatively small, the present results provide useful data about variations and distribution of the caprine PrP gene, which can be used to assess the risk of scrapie in Japan.

REFERENCES

1. Belt, P. B. G. M., Muileman, I. H., Schreuder, B. E. C., Bos-de Ruijter, J., Gielkens, A. L. J. and Smits, M. A. 1995. *J. Gen. Virol.* **76**: 509–517.
2. Billins, C., Panagiotidis, C. H., Psychas, V., Argyroudis, S., Nicolaou, A., Leontides, S., Papadopoulos, O.and Sklaviadis, T. 2002. *J. Gen. Virol.* **83**: 713–721.
3. Foster, J., Goldmann, W., Parnham, D., Chong, A. and Hunter, N. 2001. *J. Gen. Virol.* **82**: 267–273.
4. Goldmann, W., Hunter, N., Smith, G., Foster, J. and Hope, J. 1994. *J. Gen. Virol.* **75**: 989–995.
5. Goldmann, W., Martin, T., Foster, J., Hughes, S., Smith, G., Hughes, K., Dawson, M. and Hunter, N. 1996. *J. Gen. Virol.* 77: 2885–2891.
6. Goldmann, W., Chong, A., Foster J., Hope, J. and Hunter, N. 1998. *J. Gen. Virol.* **79**: 3173–3176.
7. Gombojav, A., Ishiguro, N., Horiuchi, M., Serjmyadag, D., Byambaa, B. and Shinagawa, M. 2003. *J. Vet. Med. Sci.* **65**: 75–81.
8. Hunter, N., Foster, J. D., Dickinson, A. G. and Hope, J. 1989.. *Vet. Rec.* **124**: 364–366.
9. Hunter, N., Moore, L., Hosie, B. D., Dingwall, W. S. and Greig, A. 1997. *Vet. Rec.* **140**: 59–63.
10. Ikeda, T., Horiuchi, M., Ishiguro, N., Muramatsu, Y., Kai-Uwe, G. D. and Shinagawa, M. 1995. *J. Gen. Virol.* **76**: 2577–2581.
11. Obermaier, G., Kretzschmar, H. A., Hafner, A., Heubeck, D. and Dahme, E. 1995. *J. Comp. Pathol.* **113**: 357–372.
12. Prusiner, S. B. 1991. *Science.* **252**: 1515–1522.
13. Shinagawa, M., Matsuda, A., Sato, G., Takeuchi, M., Ichijo, S. and Ono, T. 1984. *Jpn. J. Vet. Sci.* **46**: 913–916.
14. Wood, J. N. L., Done, S. H., Pritchard, G. C. and Wooldridge, M. J. A. 1992. *Vet. Rec.* **131**: 66–68.

NOTE *Public Health*

Surveillance of Chronic Wasting Disease in Sika Deer, *Cervus nippon*, from Tokachi District in Hokkaido

Natsumi KATAOKA[1)], Masakazu NISHIMURA[2)], Motohiro HORIUCHI[3)] and Naotaka ISHIGURO[4)]*

[1)]*Laboratories of Veterinary Public Health, and* [2)]*Pharmacology, Obihiro University of Agriculture and Veterinary Medicine, Obihiro, Hokkaido 080–8555,* [3)]*Laboratory of Prion Disease, Graduate School of Veterinary Medicine, Hokkaido University, Sapporo, Hokkaido 060–0813,* [4)]*Laboratory of Food and Environmental Hygiene, Faculty of Applied Biological Sciences, Gifu University, Gifu 501–1193, Japan*

(Received 3 September 2004/Accepted 24 November 2004)

ABSTRACT. Surveillance of chronic wasting disease (CWD) was conducted by performing Western blot analysis of tissue samples from 136 sika deer (*Cervus nippon*) killed by hunters in the Tokachi district of Hokkaido Island. No prion protein (PrP^{Sc}) associated with CWD was detected in any of the samples. To assess amino acid polymorphisms of the sika deer PrP gene, nucleotide sequencing of the PrP gene was performed. The only amino acid polymorphisms detected were 3 silent mutations at nucleotide positions 63, 225 and 408. These results suggest that sika deer in the Tokachi district are genetically homogeneous, and are not infected with CWD.

KEY WORDS: CWD, sika deer, surveillance.

J. Vet. Med. Sci. 67(3): 349–351, 2005

Chronic wasting disease (CWD) is a transmissible spongiform encephalopathy (TSE) of captive and free-ranging white-tailed deer (*Odocoileus Virginianus*), mule deer (*O. hemionus*) and Rocky Mountain elk (*Cervus elaphus*) in several US states and Canadian provinces [13, 15, 16]. This disease is characterized by progressive loss of body weight and abnormal behavior, and by the accumulation of a partially protease-resistant isoform (PrP^{Sc}) of a normal cellular protein (PrP^{c}) in the central nervous system. Thus, CWD is similar to scrapie in sheep and goats, and bovine spongiform encephalopathy (BSE) in cattle [1, 11]. Occurrence of CWD is currently limited to North American cervid ruminants.

Cervus nippon yesoensis, a subspecies of the sika deer (*Cervus Nippon*) that inhabit the Japanese Islands, is native to Hokkaido Island of Japan. In recent decades, the number of sika deer in Hokkaido has increased rapidly due to protection by the Hokkaido government [6]. Overpopulation of sika deer has caused immense damage to agriculture and forestry in Hokkaido.

The meat of sika deer is frequently consumed as game meat or commercially processed as ham or sausage, especially in the Tokachi district of Hokkaido Island. Although there is no evidence that CWD can be transmitted to humans, the experience of transmission of other TSEs to humans via consumption of meat or other products from ruminants raises public health concerns about the safety of sika deer meat [10, 11]. However, little is known about occurrence of CWD among sika deer on Hokkaido Island. In the present study, we used Western blot analysis to examine occurrence of CWD among sika deer killed by hunters in the Tokachi district, and determined their PrP genotypes.

We used tissue samples from 136 sika deer (82 males and 54 females) killed by hunters over a 2-year period (51 deer in 2002, and 85 deer in 2003) at 13 sites in the Tokachi district (Fig. 1). The age of the deer ranged from approximately 1 to 7 years. Samples of the obex of the medulla

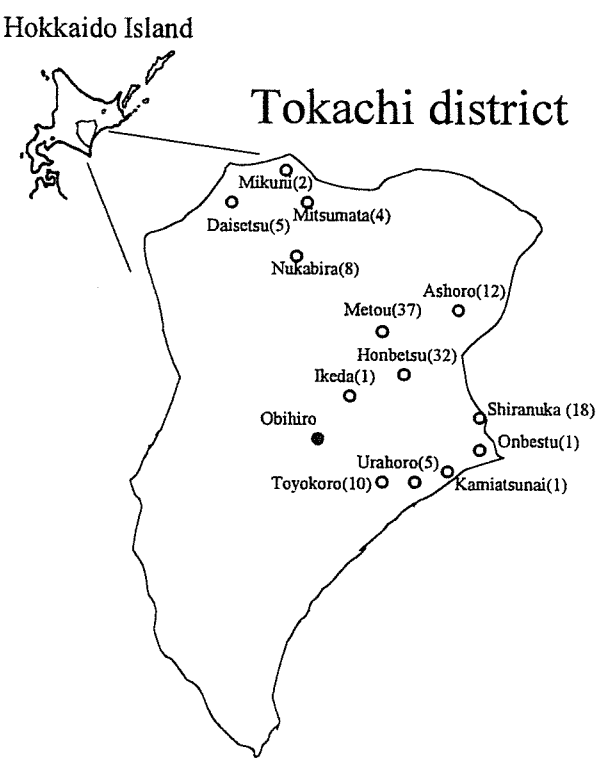

Fig. 1. Sampling sites of sika deer in Hokkaido. Tokachi district is enlarged. Numbers in parentheses are the number of sika deer killed by the hunters at each site. Obihiro city, which is indicated by a closed circle, is located at center of the Tokachi district.

* CORRESPONDENCE TO: ISHIGURO, N., Laboratory of Food and Environmental Hygiene, Faculty of Applied Biological Sciences, Gifu University, Gifu 501–1193, Japan.

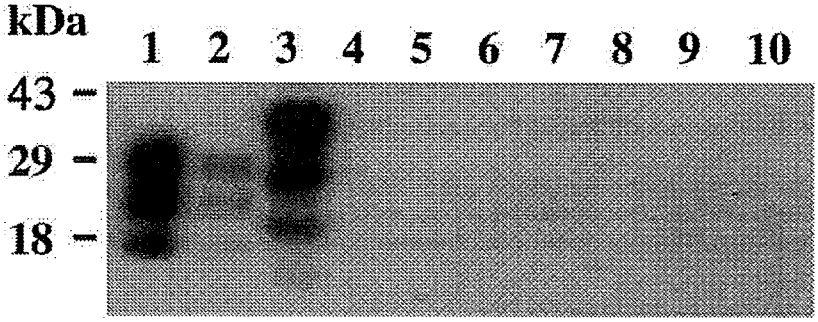

Fig. 2. Detection of PrP^{Sc} or PrP^{c} in sika deer tissue by Western blotting analysis. PrP^{c} and/or PrP^{Sc} from deer obex was prepared and dissolved in sample buffer as described previously [3]. The protein was resolved by electrophoresis in 12% polyacrylamide gels and transferred to Hybond-PVDF membranes. PrP^{Sc} and/or PrP^{c} was detected with immunoblot analysis using mAb 44B1, and was visualized using the ECL system [3]. Lane 1, PK-digested mouse PrP^{Sc} fraction of 12-μg tissue equivalent; lane 2, PK-digested mouse PrP^{Sc} fraction of 2-μg tissue equivalent; lane 3, PK-undigested PrP^{c} fraction of 2-mg tissue equivalent; lanes 4 to 10, PK-digested obex extract of 10-mg tissue equivalent. Molecular mass markers (kDa) are shown on the left.

oblongata were tested for the presence of PrP^{Sc} using Western blot analysis, and buccal muscles were tested for polymorphisms of the PrP gene by DNA sequencing. The preparation of PrP^{c} and/or PrP^{Sc} from the deer obex was performed as described elsewhere, with and without proteinase K (PK), respectively [3]. The Western blot analysis was performed as described previously, using several anti-PrP mAbs [7], and blots were developed with ECL (Amersham Buckinghamshire, England) and detected with X-ray film. PrP^{Sc} from the mouse-adapted Obihiro strain of scrapie was used as a positive control in Western blot analysis [3]. DNA was extracted from deer buccal muscle using a Dneasy Tissue Kit (Qiagen, Valencia, CA). The deer PrP gene was amplified by polymerase chain reaction (PCR) using 2 primers: BPrP3, GCAGATATAAGTCATCATGGTG; BPrP4, GGAAGGACAAAAGTGGTAGAAG [2]. The PCR products were purified using a QIAquick Kit (Qiagen), and DNA sequencing was performed as described previously [2].

To estimate the reactivity of anti-PrP mAbs to deer PrP^{c} or PrP^{Sc} molecules, the reactivity of 3 representative mAbs (132, 31C6 and 44B1, [7]) to deer PrP^{c} was examined by Western blot analysis. The mAbs 132 (which recognizes a linear epitope consisting of the amino acid sequence AVVGGLGGY) and 44B1 (which recognizes a discontinuous epitope consisting of mouse amino acid residues 155 to 231) reacted with the deer PrP^{c}, but the mAb 31C6 did not react with the deer PrP^{c} [7]. The lack of reactivity of the mAb 31C6 appears to be due to a difference in amino acid sequence between mouse and deer in the epitope region, as indicated by the DNA sequence of the deer PrP gene. Assays for deer PrP^{Sc} were performed by Western blot analysis using the mAbs 132 and 44B1. No PrP^{Sc}-specific molecules were detected in PK-treated obex extracts, although deer PrP^{c} and PrP^{Sc} from mouse-adapted scrapie (control) were observed in blots (Fig. 2).

Studies indicate that specific PrP alleles are associated with CWD in cervids [4,9]. Therefore, we examined the DNA sequences of the PrP gene in the present samples, to determine their PrP genotypes. With the exception of 3 silent mutations at nucleotide positions 63 (G→T), 255 (G→A) and 408 (C→T), the PrP sequences of the present samples were identical to the sequence with accession number AF009181 (from *Odocoileus hemionus*), and all possessed five octapeptide repeats. Specific PrP alleles were reported to be associated with CWD-positive white-tailed deer (Q^{95} G^{96} S^{138}) [4] and Rocky Mountain elk (M^{132})[9]. These amino acid sequences are observed in the wild type of sika deer PrP gene, but , it is not known if the PrP polymorphisms are associated with the occurrence of CWD in cervids on the other continents except North America [11]. No polymorphisms were observed among the present samples at the DNA level, suggesting that sika deer in Hokkaido comprise a genetically homogenous population. These results are consistent with the findings of previous mitochondrial DNA analysis [8].

There were no indications of occurrence of CWD in the present tissue samples. The number and geographical distribution of tissue samples in the present study were extremely limited. Tonsillar biopsy examined with immunohistochemical staining is a useful technique for the preclinical diagnosis of CWD in mule deer and white-tailed deer [14]. This technique might be evaluated as a practical management tool in farmed live sika deer. CWD surveillance of sika deer in the Tokachi district is important, because deer meat and other deer products are frequently consumed by humans in that area, and because sheep scrapie has been detected on farms in the Tokachi district [5, 12]. Although there is no evidence that CWD has crossed the species barrier from deer to sheep, cattle or humans [10, 11], particular care is necessary when ensuring the safety of food products

from ruminants that can carry a TSE.

ACKNOWLEDGMENTS. We wish to thank the Tokachi Hunting Club for supplying deer tissue samples. This study was supported in part by Grant-in-Aid for Scientific Research (The 21st Century Center-of-Excellence Program; E-1) from the Ministry of Education, culture, Sports, Science and Technology of Japan.

REFERENCES

1. Bolton, D.C., Mckinley, M.P. and Prusiner, S.B. 1982. *Science* **218**: 1309–1311.
2. Gombojav, A., Ishiguro, N., Horiuchi, M., Serjmyadag, D., Byambaa, B. and Shinagawa, M. 2003. *J. Vet. Med. Sci.* **65**: 75–81.
3. Gombojav, A., Shimauchi, I., Horiuchi, M., Ishiguro, N. Shinagawa, M., Kitamoto, T., Miyoshi, I., Mohri, S. and Takata, M. 2003. *J. Vet. Med. Sci.* **65**: 341–347.
4. Johnson, C., Johson, J., Clayton, M., Mckenzie, D. and Aiken, J. 2003. *J. Wildl. Dis.* **39**: 576–581.
5. Ikeda, T., Horiuchi, M., Ishiguro, N., Muramatsu, Y., Kai-Uwe, G.D. and Shinagawa, M. 1995. *J. Gen. Virol.* **76**: 2577–2581.
6. Kaji, K. 1995. *Honyurui Kagaku (Mammalian Science)* **35**: 35–43 (in Japanese).
7. Kim, C-L., Umetani, A., Matsui, T., Ishiguro, N., Shinagawa, M. and Horiuchi, M. 2004. *Virology* **320**: 41–52.
8. Nabata, D., Masuda, R. and Takahashi, O. 2004. *Zool. Sci.* **21**: 473–481.
9. O'Rourke, K.I., Besser, T.E., Miller, M.W., Cline, T.F., Spraker, T.R., Jenny, A.L., Wild, M. A., Zebarth, G.L. and Williams, E.S. 1999. *J. Gen. Virol.* **80**: 2765–2769.
10. Raymond, G.J., Bossers, A., Raymond, L.D., O'Rourke, K.I., McHolland, L.F., Bryant III, P.K., Miller, M.W., Williams, E.S., Smits, M. and Caughey, B. 2000. *EMBO J.* **19**: 4425–4430.
11. Salman, M.D. 2003. *J. Vet. Med. Sci.* **65**: 761–768.
12. Shinagawa, M., Matsuda, A., Sato, G., Takeuchi, M., Ichijo, S. and Ono, T. 1984. *Jpn. J. Vet. Sci.* **46**: 913–916.
13. Spraker, T.R., Miller, M.W., Williams, E.S., Getzy, D.M., Adrian, W.J., Schoonveld, G.G., Sponwart, R.A., O'Rourke, K.I., Miller, J.M. and Merz, P.A. 1997. *J. Wildl. Dis.* **33**: 1–6.
14. Wild, A.M., Spraker, R. T., Sigurdson, J. C., O'Rourke, I. K. and Miller, W. M. 2002. *J. Gen. Virol.* **83**: 2629–2634.
15. Williams, E.S. and Young, S. 1980. *J. Wildl. Dis.* **16**: 89–98.
16. Williams, E.S. and Young, S. 1982. *J. Wildl. Dis.* **18**: 465–471.

特集 プリオン病

2．BSE診断法の開発と現状

堀内 基広
北海道大学大学院獣医学研究科 プリオン病学講座 教授

伝達性海綿状脳症（プリオン病）の病原体“プリオン”は，病原体特異的な核酸を持たず，主要構成要素は異常型プリオン蛋白質（PrP^{Sc}）である。病原体のゲノムに相当する核酸を持たないので，PCRによる病原体遺伝子の増幅はプリオン検出に応用できない。PrP^{Sc}は宿主遺伝子PrPの産物あるためプリオンに対する免疫応答は起こらない。従って，血清診断も応用できない。現状では，中枢神経系組織からPrP^{Sc}を検出することにより確定診断される。これまでに，複数のBSE検査キットが販売されているが，全てPrP^{Sc}検出を指標にしている。ヒトプリオン病では，14-3-3などが髄液中の蛋白質が診断補助マーカーとして使用されており，MRIが早期診断に有用であることが明らかとなってきたが，BSEをはじめとする動物プリオン病では，有用な診断補助マーカーはない。と畜前の生前検査を可能にするためには，PrP^{Sc}検出の高感度化とともに診断補助マーカーの探索も重要な課題である。

Key Words：プリオン／牛海綿状脳症／診断法／異常型プリオン蛋白質

Development of BSE diagnosis methods and its current situation

Motohiro Horiuchi

Laboratory of Prion Diseases, Graduate School of Veterinary Medicine, Hokkaido University Professor

The causative agent of transmissible spongiform encephalopathies (TSEs, prion diseases), called “prion”, is thought to lack specific nucleic acids as a genome, and the major component of prion is believed to be an abnormal isoform of prion protein (PrP^{Sc}). Since prion has no agent-specific nucleic acids, amplification of gene by PCR cannot be applicable for the detection of prion. In addition, it is difficult to disclose prion infected animal by serum diagnosis because PrP^{Sc} in encoded by host gene PrP and thus no immune response against PrP^{Sc} is induced in prion-infected animals. Conclusive diagnosis of BSE is mainly made by the detection of PrP^{Sc} in the central nervous system. In human prion diseases, certain proteins in cerebrospinal fluid such as 14-3-3, S100, and neuron-specific enolase, are now being used as surrogate markers. In addition, magnetic resonance imaging is useful for diagnosis of prion-affected patients in early clinical phase. However, no useful disease-specific markers have been developed in animal prion diseases. To accom-

plish an ante mortem diagnosis of BSE and other animal TSEs, it is important to develop ultra-high sensitive PrP^{Sc} detection methods and to find out reliable surrogate markers.

Key Words : prion ／ BSE ／ diagnosis ／ PrP^{Sc}

プリオン検出の概念

細胞変性効果(CPE)やプラークにより，ウイルスを検出したり，感染価（infectious dose；ID）を定量することができる。あるいは動物に接種して動物を致死させる量（lethal dose；LD）として定量化する場合もある。一方，プリオンは培養細胞では増殖効率が悪いために，培養細胞を用いた感染価の測定は難しい。

現在，プリオンの検出法として主に，1）プリオンの構成要素である PrP^{Sc}（異常型プリオン蛋白質）を免疫生化学的手法により検出する，2）被検試料を実験動物に接種して病気の伝播を確認するバイオアッセイ，の2つの方法が用いられている。PrP^{Sc} の検出は，プリオンの構成要素の検出により間接的にプリオンの存在を判断するもので，プリオン病の確定診断に広く用いられている。バイオアッセイはプリオンの生物活性を指標にしている。

プリオン特異的な核酸は発見されていないので，PCR（polymerase chain reaction）による病原体特異的核酸の増幅は応用できない。また，PrP^{Sc} は宿主遺伝子 PrP(プリオン蛋白質)の産物であり，正常型プリオン蛋白質（PrP^{C}）と同一のアミノ酸配列を有することから，プリオン病罹患動物では PrP^{Sc} に対する免疫応答がない。従ってプリオン病罹患者・動物の血清診断はできない。

PrP^{Sc} 検出法の原理（図1）

正常な動物の脳組織には PrP^{C} が発現している。一方，プリオンに罹患した動物の脳には PrP^{C} と PrP^{Sc} の両方が存在する。免疫生化学的な PrP^{Sc} 検出は，抗 PrP 抗体により PrP^{Sc} を特異的に検出するものと誤解されることがあるが，使用する抗 PrP 抗体は PrP^{C} と PrP^{Sc} の両方に反応する。より正確には，抗体は変性剤処理した PrP^{C} と PrP^{Sc} の両方に反応するので，抗 PrP 抗体では両者を区別できない。従って，試料調製の段階で PrP^{C} を除去しておく必要がある。実際には，PrP^{Sc} と PrP^{C} の蛋白質分解酵素感受性の差を利用して，Proteinase K(PK)処理により PrP^{C} を除去する。PrP^{Sc} は凝集体を形成しており，抗 PrP 抗体が認識するエピトープを露出していないので，凝集体を変性剤処理して PrP^{Sc} を変性させる。ELISA(enzyme-linked immunosorbent assay）ではグアニジン塩酸塩や尿素などで，ウエスタンブロット(WB)では SDS(sodium dodecyl sulfate)により PrP^{Sc} を変性させる。変性後の PrP^{Sc} を抗 PrP 抗体を用いて検出する。免疫組織化学では，切片を蒸留水に浸した状態で 121 ℃，20 分オートクレーブ処理することで，PrP^{Sc} が部分的に変性しエピトープが露出すると考えられる（hydrizing autoclave 法）[1]。使用する抗 PrP 抗体の種類にもよるが，この処理は，135℃，2 気圧というさらに厳しい条件がより効果的との知見も得られている[2]。

BSE 迅速検査用キットの評価

1998 年にチューリッヒ大学からスピンオフされたプリオニクス社が，世界初の BSE（bovine spongiform encephalopathy)検査キット“Pronics-Check”を販売した。WB による BSE 検査キットで，1999 年にはスイスではこれを用いて BSE 検査が開始された。その後，Bio-Rad 社，Enfer 社が，BSE 検査キットを発売し，2000 から 2001 年にかけて EU 諸国で BSE 検査が実施されるようになった。EC ではこれまでに，3 度 BSE の迅速検査法の評価を実施している（表1）。第一回の評価では 4 キット，第二回目は 5 キット，第三回では 10 キットが評価を受けた[3～5]。第三回目の実

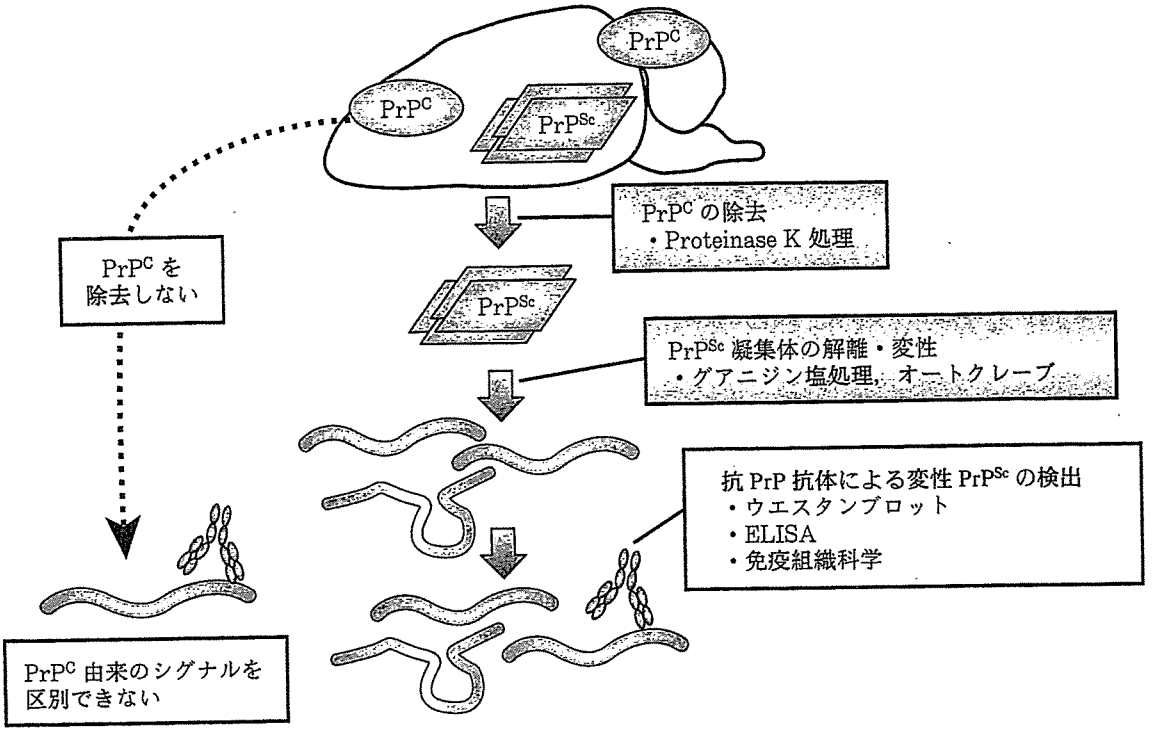

図1 PrP^Sc 検出の原理

PrP^Sc は凝集しているため，抗 PrP 抗体で検出するためには，一度変性させる必要がある。PrP^C 由来の分子に対する抗体の反応，PrP^Sc 由来の分子に対する抗体の反応を区別することが出来ないので，変性前に PrP^C の除去が必須である。

施例では，キットの基本性能を試験するフェーズⅠ試験は，1）感度（diagnostic sensitivity）：BSE 臨床例 50 検体中陽性と判定した割合，2）特異性（diagnositic specificity）：BSE 陰性例 150 検体中陰性と判定した割合，3）検出限界（Detection limit）：BSE 陽性牛の脳を陰性牛の脳で希釈した希釈列（1：5，1：50，1：100，1：200）の検出限界，の 3 種の試験から成る。フェーズⅠ試験をクリアすると，10,000 程度の検体，および 200 程度の質の劣化した検体を用いるフィールド試験に進む。これまでに 12 キットがフィールド試験を終了して，EC（現在は European Food Safety Authority；EFSA）の承認を受けている。第三回の評価では日本の企業(富士レビオ株式会社)がエントリーして，フェーズⅠ試験では良好な成績を得て，フィールド試験へ進んでいる。

これまでに開発されたキットは，ウエスタンブロット（Prionics-Check WB），2 種の抗体を使用する sandwich-ELISA で抗原抗体複合体を，i）発色試薬で検出（Platelia BSE Kit, FRELISA BSE など），ii）化学発光試薬で検出（Prionics-Check LIA，Institut Pourquier Speed'it など），iii）あるいは時間分解蛍光測定で検出(CDI)，PrP^Sc を選択的に結合するポリマーを使用した直接 ELISA（Enfer BSE Kit, IDEXX HerdCheck BSE Atigen Test Kit), filter-ELISA(CediTect BSE test)，イムノクロマト法(Prionics-Check PrioSTRIP）に大別される（表 1）。

各々のキットにはそれぞれ特徴がある。Platelia BSE Kit は試料調整の簡便化に成功した一例である。Enfer BSE Kit や IDEXX HerdChech BSE は PrP^Sc を選択的に結合する化学物質をコートしたプレートを使用している点が特徴である。IDEXX 社のキットでは Microsens Biotechnology 社がライセンスを有する Seprion と呼ばれる化学ポリマーを使用している。この化学ポリマーは PrP^Sc に対する選択性が高いらしく，IDEXX 社のキットでは試料調整に PK を使用していない。全ての PrP^Sc が蛋白質分解酵素抵抗性ではなく，PK 処理により分解される PrP^Sc も存在する。従って，PK 処理を省くことでより多くの PrP^Sc が残存し，

表1　EC による BSE 迅速検査キットの評価

	会社など	キット名	原理／特徴	検出法	検出限界
第一回（1999 年）4 社	Prionics, Switzerland	Prionics-Check WB	WB	化学発光	10^{-1} (15/20)
	Enfer Technology, Ireland	Enfer TSE Kit	直接 ELISA	化学発光	$10^{-1.5}$ (20/20)
	CEA (Bio-Rad), France	Platelia BSE detection Kit	Sandwich-ELISA	発色	$10^{-2.5}$ (18/20)
第二回（2002 年）5 社	ID Lelystad, Netherlands	NA	Filter-assay／変性・未変性測定	化学発光	1：81 (4/4)
	Prionics, Switzerland	Prionics-Check LIA	Sandwich-ELISA	化学発光	1：243 (2/4)
	USDA (InPro), USA	aCDI	Sandwich-assay／変性・未変性測定 /PTA 沈殿	時間分解蛍光	$10^{-2.0}$ (2/4)
	MRC prion unit, Imperial College, UK	NA	Sandwich-assay	電子化学発光	1：270 (10/12)
第三回（2004 年）10 社	CEDI Diagnostic, Netherlands	CediTect BSE test	Filter-assay／変性・未変性測定	化学発光	＞1：200 (5/6)
	Fujirebio, Japan	FRELISA BSE	Sandwich-ELISA	発色	＞1：200 (6/6)
	IDEXX Laboratories, USA	IDEXX HerdChek BSE Antigen Test Kit, EIA	直接 ELISA/PK 処理無	発色	1：800 (5/6)
	Institut Pourquier, France	Institut Pourquier Speed'it BSE	Sandwich-ELISA	化学発光	1：64 (4/5)
	Labor Diagnostik Leipzig GmbH, Germany	Priontype *post mortem*	Sandwich-ELISA/PK 処理無	発色	1：25 (4/4)
	Prionics, Switzerland	Prionics-Check PrioSTRIP	Lateral flow	目視	1：100 (16/16)
	Roboscreen GmbH, Germany	Roboscreen Beta Prion BSE EIA Test Kit	Sandwich-ELISA	発色	＞1：200 (6/6)
	Roche Diagnostics GmbH, Germany	Roche Applied Science PrionScreen	Sandwich-ELISA	発色	1：100 (10/12)
	Enfer Scientific, Ireland	Enfer TSE Kit v2.0 (autom. Sample prep.)	直接 ELISA	化学発光	＞1：200 (10/12)

第一回から第三回まで，エントリーしたキットの中で，感度と特異性をクリアしたキットのみ表に示した。

それを選択的に回収可能ならば，検出感度の上昇につながる。CDI と CediTect BSE test では，PrP^{Sc} を変性および未変性の条件で抗体との反応性を解析している点が特徴である。PrP^{Sc} は未変性条件下では抗 PrP 抗体のエピトープをあまり露出していないが，変性に伴いエピトープが露出し，抗体の反応性が上昇する。変性・未変性条件下で構造の変化に伴う抗体の反応性の差を測定することで S/N 比の向上が見込まれる。In-Pro 社はこの特徴から“CDI（conformation dependent immunoassay）”と呼んでいる。CDI では，変性・未変性で測定する点を利用して，低濃度の PK を行い過剰な PrP^{Sc} の分解を避けている。PrP^{Sc} の濃縮にリンタングステン酸（PTA）を使用した点も CDI の特徴の一つである。PrioSTRIP はラテラールフロー法を使用しているが，EC の評価では検出限界が 1：100 程度と良好であることも注目に値する。

現在の技術水準では，感度および特異性は 100%一致することは最低条件であり，検出限界がキットの性能を見極める判断材料となる。第一回，二回の評価では，10^{-3} 以上の希釈列で検出限界を判断することができたが，第三回の評価では一部例外はあるが，原則希釈列を 10^{-2} までしか使用していないので真の検出限界を知ることは出来ない。三回の評価報告を総合的に判断すると，良好な検出限界を示すキットは 1：200 以上の希釈でも陽性の反応を呈している。つまり，BSE 発症牛の延髄に蓄積している PrP^{Sc} の 1/200 程度の量の PrP^{Sc} が蓄積している感染牛を摘発可能な感度を有している。

我が国の BSE 確認検査と迅速検査キットの検出限

現在，我が国では，Platelia BSE Kit(Bio-Rad 社)，